© 2016. Published by The Company of Biologists Ltd | Journal of Experimental Biology (2016) 219, 1639-1648 doi:10.1242/jeb.127886

RESEARCH ARTICLE

Whiteflies stabilize their take-off with closed wings

Gal Ribak[1,2,*], Eyal Dafni[1] and Dan Gerling[1]

ABSTRACT

The transition from ground to air in flying animals is often assisted by the legs pushing against the ground as the wings start to flap. Here, we show that when tiny whiteflies (*Bemisia tabaci*, body length ca. 1 mm) perform take-off jumps with closed wings, the abrupt push against the ground sends the insect into the air rotating forward in the sagittal (pitch) plane. However, in the air, *B. tabaci* can recover from this rotation remarkably fast (less than 11 ms), even before spreading its wings and flapping. The timing of body rotation in air, a simplified biomechanical model and take-off in insects with removed wings all suggest that the wings, resting backwards alongside the body, stabilize motion through air to prevent somersaulting. The increased aerodynamic force at the posterior tip of the body results in a pitching moment that stops body rotation. Wing deployment increases the pitching moment further, returning the body to a suitable angle for flight. This inherent stabilizing mechanism is made possible by the wing shape and size, in which half of the wing area is located behind the posterior tip of the abdomen.

KEY WORDS: Flight stability, Jumping, Pitch, Tumbling, Wing deployment

INTRODUCTION

When flying animals take off, the lift produced needs to overcome the weight of the flyer and accelerate the body upwards. The maximal upwards acceleration should be limited by the aerodynamic performance of the wings and the maximal power output of the flight muscles (Marden, 1987). However, pushing against the ground with the legs can be used to achieve steeper and/or faster take-offs (Bimbard et al., 2013; Pond, 1972; Provini et al., 2012). The contribution of the leg thrust for take-off may range from 0% in animals that rely solely on the wings (e.g. rhinoceros beetles; Van Truong et al., 2014), to 59% in hummingbirds (Tobalske et al., 2004), which use both legs and wings, and up to 100% in animals that launch themselves by jumping into the air with the wings folded next to the body (e.g. grasshoppers; Pond, 1972).

Flight initiation by jumping is particularly interesting in insects, because within the animal kingdom, arthropods hold the record in jump performance relative to their small body size (Schmidt-Nielsen, 1997). Insects such as fleas (Bennet-Clark and Lucey, 1967), grasshoppers (Bennet-Clark, 1975; Heitler, 1974), leafhoppers (Burrows, 2007), flea beetles (Furth et al., 1983), click beetles (Evans, 1972) and many more (see review in Burrows and Dorosenko, 2014) can launch their body into the air, covering distances of tens of body lengths in a single jump. To increase the speed at leaving the ground, some insects push their body off the ground with extremely high acceleration, reaching up to 300–400 times the gravitational acceleration (e.g. click beetles and froghoppers; Burrows, 2003; Evans, 1972). To provide the high power needed for these accelerations, these insects rely on elastic energy (Gronenberg, 1996; Patek et al., 2011). In such jumps, muscles contract slowly to perform mechanical work on an elastic element of the skeleton. The elastic element serves as a spring, storing the mechanical work, until a trigger mechanism abruptly unleashes the stored elastic energy, launching the insect into the air at striking accelerations (reviewed by Gronenberg, 1996).

If the abrupt ground reaction force, which is generated during the jump, does not pass exactly through the center of mass, a high torque will ensue, sending the insect tumbling into the air. Indeed, vigorous rotations (10–400 revolutions s^{-1}) in the air have been described in jumping insects that propel their jump elastically (e.g. flea beetles; Brackenbury and Wang, 1995; springtails; Burrows, 2012; jumping plant lice; Christian, 1978). Because it is difficult to avoid the torque generated during take-off, insects that jump to initiate flight should be able to correct body orientation during the transition from jumping to stable flapping flight (Brackenbury and Wang, 1995; Card and Dickinson, 2008). With their wings spread out, insects can use their wings to dynamically correct for perturbations in their body orientation (Dickinson, 1999; Ristroph et al., 2010, 2013), enabling them to aerodynamically stabilize the orientation of their body. However, when the take-off is performed with the wings placed in the resting position, the ability to control body orientation in air may be limited.

We investigated how whiteflies cope with this problem during their take-off jumps with closed wings. Whiteflies (Hemiptera: Aleyrodidae) are notorious agricultural pests, and their biology and flight behavior have been studied extensively (Blackmer and Byrne, 1993; Byrne, 1991; Isaacs et al., 1999). However, with the exception of one qualitative description (Weber, 1931, see Discussion), very little work has been done on their flight initiation mechanism. While working on the take-off of the tobacco whitefly, *Bemisia tabaci* (Gannadius 1889) (adult body length ca. 1 mm), we noticed that they launch their body into the air by jumping with their wings held against the sides of the body in the resting position. The wings are elevated to the dorsal position, in preparation for the first downstroke, only after the body had moved several body lengths through the air (Movie 1). The jumps are abrupt and powerful (see Results), suggesting that whiteflies exploit elastic energy for jumping.

We hypothesized that the powerful take-off jumps pose a challenge to stabilizing body orientation, and that the long wings, in their resting position, act in the air to stabilize body orientation prior to wing deployment and the initiation of flapping flight. To test this hypothesis, we recorded whitefly take-off using high-speed cameras. We then analyzed the resulting movies to time wing deployment and body rotation during the transition from the ground to flapping flight. We expected to find in each take-off incident one of the following scenarios. (1) Whitefly transition from ground into air without substantial rotation of the body, indicating that whiteflies

[1]Department of Zoology, Faculty of Life Sciences, Tel Aviv University, Tel Aviv 6997801, Israel. [2]Sagol School of Neuroscience, Tel Aviv University, Tel Aviv 6997801, Israel.

*Author for correspondence (gribak@post.tau.ac.il)

Received 27 October 2015; Accepted 8 March 2016

Journal of Experimental Biology (2016) 219, 1639-1648 doi:10.1242/jeb.127886

List of symbols and abbreviations

a	average linear acceleration of the body during the 'acceleration' phase
A	area of the wings
A'	proportion of wing area projected as frontal area (projected onto a plane perpendicular to the direction of motion)
BE	blade element
B_L	body length (not including wings)
C_D	aerodynamic drag coefficient
C_f	skin friction coefficient
C_F	aerodynamic force coefficient
C_L	aerodynamic lift coefficient
C_p	torque coefficient for pitch
C_s	rotational damping
d_p	equivalent spherical diameter
F_n	aerodynamic force on the nth wing element
H	3D position of the tip of the head in each movie frame
I_{yy}	the mass moment of inertia for rotation about the pitch axis at the center of mass
K	drag coefficient of a plate in normal flow
l	longitudinal major axis of an ellipse/cylinder
m	body mass
$\mathbf{r}$	vector connecting the centroid of a wing section with the center of mass.
R	wing length
Re	Reynolds number
t	body thickness (minor axis of an ellipse)
T	3D position of the anterior tip of the abdomen in each movie frame
t_0	instant in the movies where the whiteflies start to accelerate for take-off
t_1	instant in the movies where the whiteflies leave the ground
t_2	instant in the movies where the wings start to supinate
t_3	instant in the movies where the wings start to elevate
t_4	instant in the movies where the wings start to flap (first downstroke)
U	velocity relative to air
$\mathbf{V}_0$	velocity at leaving the ground (take-off velocity)
V_{0h}	horizontal component of $\mathbf{V}_0$
V_{0v}	vertical component of $\mathbf{V}_0$
w	diameter of an ellipsoid in the transverse axis
α	angle-of-attack of a wing element
β	angle of incidence (measured in the sagittal plane)
γ	jump angle relative to the horizontal ground
ε	supination angle of the wings in the resting position
θ	pitch angle of the longitudinal axis of the body
$\dot{\theta}$	rotation rate (angular velocity) for pitch
$\dot{\theta}_w$	rotation rate (angular velocity) of the wing about the pitch axis
$\ddot{\theta}$	angular acceleration for pitch
μ	dynamic viscosity of air at room temperature (1.84×10^{-5} kg m^{-1} s^{-1})
ρ	density of air at sea level and room temperature (1.2 kg m^{-3})
τ_b	aerodynamic torque due to the body (without the wings)
τ_w	aerodynamic torque due to the wings
ϕ	wing elevation angle

push against the ground in a stable manner that prevents body rotation during the transition from ground into air. (2) Whiteflies tumble in the air immediately after the take-off jumps, stopping the rotation of the body only after the wings are deployed and flapped. This would indicate that a destabilizing torque is generated as the insect pushes against the ground, and that the insect relies on the aerodynamics of the flapping wings to stabilize body rotation. (3) Whiteflies leave the ground tumbling but stop or slow down the body rotation considerably prior to wing deployment and flapping. This would suggest that destabilizing torques are generated during pushing against the ground, but also that once the body is in the air, aerodynamic counter-torques, generated from the motion of the body through air, stabilize body rotation prior to wing deployment. Such counter torques can result from longitudinal static-stability where aerodynamic forces acting on the body and wings at a distance from the center of mass result in aerodynamic counter-torque when the insect rotates (pitch) from a stable orientation (Ribak et al., 2013; Thomas and Taylor, 2001). To evaluate the contribution of the wings (in the resting position) to stabilization of body orientation in the air, we observed the rotational dynamics at take-off of whiteflies with clipped wings.

MATERIALS AND METHODS

Insects

Tobacco whiteflies, *Bemisia tabaci* biotype MEAM1 (Fig. 1), were collected using an aspirator from a population maintained at Tel Aviv University in a greenhouse on collard (*Brassica oleracea acephala*) plants. The insects were transferred to glass vials and transported to the laboratory for testing within the same day. Morphological data were obtained from measurements taken from photographs of cooled whitefly adults, using a camera mounted on a dissecting microscope (Wild M40, magnification ×50). Body dimensions were measured in the images. Forewing length, area and center of area were calculated from the wing's contour in the images, as in Ribak et al. (2009).

Capturing take-offs with high-speed cameras

To capture the rapid take-offs, we used two high-speed cameras (Fastcam SA3, Photron Inc.) positioned orthogonally, filming at 2000 or 3000 frames s^{-1}. An additional filming session at 6000 frames s^{-1} focused on the action of the insects on the ground (see below). To provide light for high-speed photography, two near-infrared LED arrays were pointed at the cameras, providing backlight illumination to the filmed whiteflies. The glass vial containing the insects was placed between the lights and the cameras, and was covered by a flat glass lid, leaving only a small opening for the whiteflies to exit the vial. When a whitefly from inside the vial found the small opening in the lid and passed through it, it typically walked on the upper side of the lid for a short period, then paused and took-off. In total, we recorded take-offs from 148 whiteflies.

Take-off analysis from films

First, we observed the take-off of 100 whiteflies. Most (91%, see Results) of the whiteflies took off in a jump with their wings in the resting position. The transition from ground to flapping flight followed a pattern consisting of several components in a sequence (referred to as 'acceleration', 'ballistic', 'supination' and 'elevation' phases in Fig. 2). First, the insect paused motionless on the ground. Then, in the 'acceleration' phase, the center of mass accelerated to take-off velocity (velocity at leaving the ground) as the hind legs pushed against the ground. Next, in the 'ballistic' phase, the body moved through the air with the wings in their resting position. In the next phase, wing deployment started with a supination of the wings, while the wings are still pointing backwards. Supination continued until the plane of the wings became parallel to the frontal (dorsal) plane of the body (Fig. 2A). Finally, in the 'elevation' phase, the wings were elevated about their joints to the dorsal stroke reversal point without moving sideways. Once the wings reached that

Journal of Experimental Biology

Journal of Experimental Biology (2016) 219, 1639-1648 doi:10.1242/jeb.127886

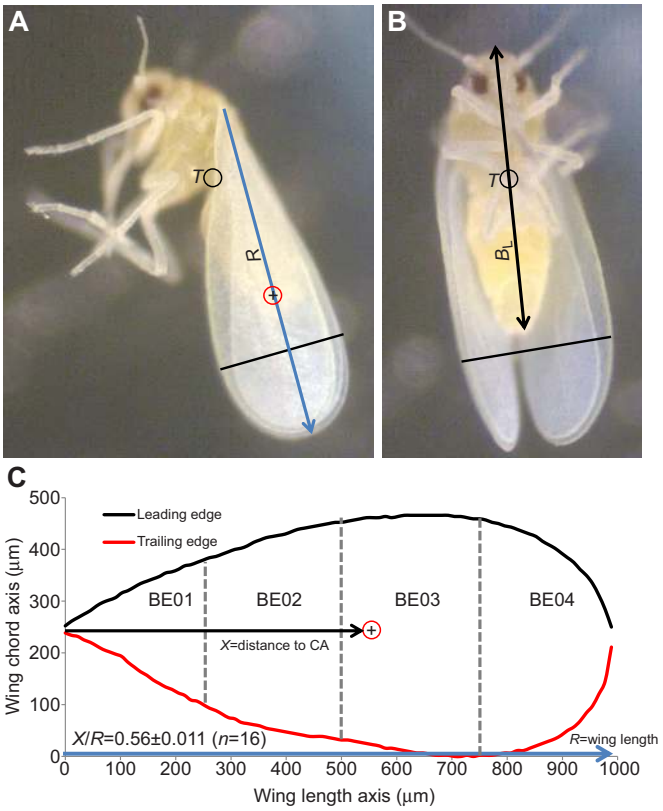

Fig. 1. The study species, *Bemisia tabaci*. (A) Side and (B) ventral views. The black circle with a '*T* denotes the estimated position of the center of mass and the black line denotes the maximal wing chord. The blue arrow in A denotes wing length (*R*) and the black arrow in B denotes the body length (B_L). (C) Measurement of wing shape and size. The geometric center of wing area (CA) is denoted by a red circle with a '+' in A and C. Dashed gray lines in C illustrate the spanwise division of the wing into four elements (BE01–04) for the blade-element analysis.

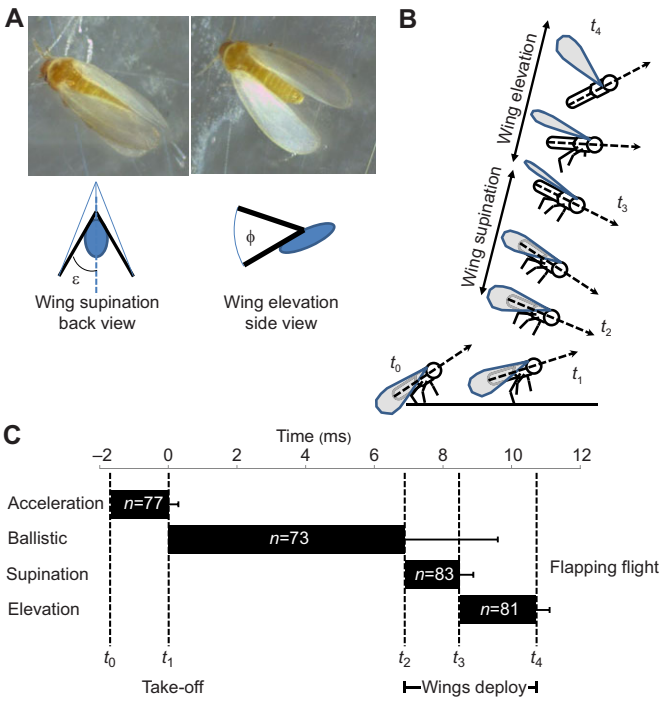

Fig. 2. The take-off sequence. (A) Definition of the wing supination (ε) and elevation (ϕ) angles and two planform (dorsal) views of whiteflies demonstrating how different supination angles change the projected area of the wings onto a frontal plane. (B) An illustration (not to scale) showing the definition of different phases in the take-off sequence. The instant that the insect on the ground starts to move is t_0. The instant it leaves the ground is t_1. While airborne, at t_2 the wings start to supinate, at t_3 they start to elevate and at t_4 they start to flap. Dashed arrows denote the longitudinal axis of the body. (C) Timing of the various phases in the take-off sequence as measured in the videos. Horizontal columns represent mean duration and error bars are ±1 s.d.

position, they pronated and moved down in the first downstroke (supplement film 1). Time allocation between these phases was measured by finding the following time points in the take-off sequence (Fig. 2): (t_0) the first movement of the body during the acceleration phase; (t_1) the instant the last leg left the ground; (t_2) the instant the wings started supinating from their position at rest (along the sides of the body); (t_3) the instant at which the wings in the frontal plane started to elevate; and (t_4) the instant at which the wings reached the final dorsal position and started to pronate in preparation for flapping. Time points t_0 and t_1 defined the duration of the 'acceleration' phase; t_1 and t_2 defined the duration of the 'ballistic' phase; and t_2 and t_4 defined the duration of 'wing deployment', which could be sub-divided to: 'supination' (t_2–t_3) and 'elevation' (t_3–t_4). The acceleration phase proved to be very short (1.7 ms, see Results). Therefore, to confirm its duration with improved temporal resolution, we filmed the take-offs of another 14 whiteflies at 6000 frames s^{-1}.

In 34 take-off movies, we determined the kinematics of the body after leaving the ground. The cameras were synchronized to record simultaneously and were spatially calibrated, thus allowing us to extract the 3D position of points on the body (Hedrick, 2008). In each movie frame we identified a point (*T*) on the longitudinal axis of the body, at the connection between the thorax and abdomen (Fig. 1A,B). We used *T* as an approximation for the position of the center of mass in air. The speed (at leaving the ground) and direction (elevation angle relative to the horizontal ground) of each take-off were found by regression of the instantaneous horizontal and vertical positions of *T* over time (time interval between frames). From the least-square-error equations (second-order polynomial, $r>0.96$ for all cases) we found the derivative at t_1 to give the take-off velocity ($\mathbf{V}_0$) of the insects. The take-off angle (γ) was calculated as:

$$\gamma = \tan^{-1}\left(\frac{V_{0v}}{V_{0h}}\right), \quad (1)$$

where V_{0v} and V_{0h} are the vertical and horizontal components of the take-off velocity, respectively. The average acceleration of the body from rest to $\mathbf{V}_0$ was found from the acceleration duration, as:

$$a = \frac{|\mathbf{V}_0|}{t_1 - t_0}. \quad (2)$$

During the take-off jumps, the whiteflies left the ground rotating about the pitch axis (see Results). When the take-off was performed from a tilted surface they rotated more vigorously and about all three axes (compare Movies 1 and 2). To exclude these cases from the analysis of body rotation, we only used 32 films in which the whiteflies were clearly seen standing away from the edges of the lid. This ensured that in the starting position of these take-offs, the legs were resting against the same flat and horizontal glass surface. In these movies we also identified the position of the head (*H*, marked between the bases of the antennae). Points *H* and *T* were used to measure the instantaneous angle (θ) between the longitudinal axis of

the body and the horizontal plane (hereafter 'pitch angle') using:

$$\theta = \sin^{-1}\left(\frac{Hz - Tz}{\sqrt{(Hx - Tx)^2 + (Hy - Ty)^2 + (Hz - Tz)^2}}\right), \quad (3)$$

where x, y and z denote the coordinates of T and H on the lab-based XYZ axes, where Z is vertical and positive when pointing up. Image resolution in the movies sets a limit to the accuracy of the measurement of θ. The minimal measurement error in each of the movies was on average 2.8 deg (s.d.=0.76 deg, n=34).

In 13 movies, the orientation of the insects relative to the cameras allowed us to measure wing supination and elevation during the wing deployment phase. In each film frame we measured the instantaneous wing supination angle (ε) and wing elevation angle (ϕ, as defined in Fig. 2A). The elevation angle, instantaneous body pitch angle (θ), and jump angle (γ) gave the angle of incidence (β), measured between the wing length and direction of linear motion relative to air. The supination and incidence angles were used to calculate the proportion of wing area projected as frontal area onto the air flow as:

$$A' = \sin\varepsilon \sin\beta, \quad (4)$$

where A' is a non- dimensional number between 0 and 1. A value of A'=1 indicates that the entire wing area is in a plane perpendicular to the direction of motion.

Take-off with clipped wings

To empirically test the significance of the closed wings in aerial righting, we filmed additional whiteflies taking off, either after their wings were entirely removed or after removing the distal half of the wing length. To cut the wings, the insects were immobilized by cooling to 4°C. Because of their small size and delicate bodies, it proved extremely difficult to cut the wings of whiteflies without injuring them. Furthermore, the uninjured whiteflies were reluctant to jump after their wings were clipped. As a result, we were only able to record the jumps of 34 uninjured insects and each cooperating insect was allowed to take off more than once. This resulted in 13 usable take-offs by seven whiteflies with wings removed and 10 usable take-offs by nine whiteflies with clipped distal wing sections. In movies showing insects with clipped wings, we identified all the take-off phases described above. In movies showing wingless whiteflies, we only differentiated between the 'acceleration' and 'ballistic' phases, with the latter continuing until the insect left the field of view of both cameras.

Biomechanical model

To evaluate whether aerodynamic force on the closed wings and body can resist the (forward) pitching rotation of the body in the air, we used a simplified biomechanical model based on the quasi-steady, blade-element approach. The model deals only with the aerial phase of the take-off jump, i.e. the period after the insects leave the ground and prior to the initiation of wing flapping.

The angular deceleration in the pitch plane is expressed as:

$$I_{yy}\ddot{\theta} = \tau_{\text{pitch}} = \tau_w + \tau_b + C_s\dot{\theta}, \quad (5)$$

where I_{yy} is the moment of inertia for rotation about the pitch axis passing through the center of mass, τ_w is the aerodynamic torque of the closed wings, τ_b is the aerodynamic torque on the body moving with its longitudinal axis at an angle to the direction of motion, C_s is the rotational damping coefficient of the body and $\dot{\theta}$ and $\ddot{\theta}$ are the angular velocity and angular acceleration for the pitch rotation, respectively.

For I_{yy}, we used the mass moment of inertia of two ellipsoids, one representing the head+thorax, and the other representing the abdomen. Each ellipsoid had the maximal body thickness (t) and half the body length (l) as major axes. The two ellipsoids are connected by their longitudinal axes and the moment of inertia is calculated relative to the point of contact between the two ellipsoids (the center of mass). The moment of inertia then becomes:

$$I_{yy} = \frac{m(1.5l^2 + t^2)}{20}, \quad (6)$$

where m is the total mass of the body.

Next, we calculated the rotational damping coefficient of the body as in Fry et al. (2003), using the body dimensions and an integration of Stokes' law:

$$C_s = \frac{\pi\mu l^3}{3\ln(l/2t)}, \quad (7)$$

where μ is the dynamic viscosity of air (1.84×10^{-5} kg m^{-1} s^{-1}).

The pitching moment on the ellipsoid body due to fluid force was obtained, for intermediate Reynolds number ($10<Re<50$), based on published coefficients derived for small ellipsoids using direct numerical simulations (Zastawny et al., 2012):

$$\tau_b = \frac{1}{2}\rho\frac{\pi}{8}d_p^3U^2C_p, \quad (8)$$

where ρ is the density of air (1.2 kg m^{-3}), U is the velocity of the body, d_p is the equivalent diameter for a spherical body with the same volume as the ellipsoid and C_p is the torque coefficient.

The equivalent diameter is found from the axes of the ellipsoid:

$$d_p = \sqrt[3]{ltw}, \quad (9)$$

where w is the transverse axis (diameter).

C_p is a function of the Reynolds number (Re) and the angle of incidence (β) between the longitudinal axis and the direction of motion. From Zastawny et al. (2012):

$$C_p = \frac{2.078}{Re^{0.279}} + \frac{0.372}{Re^{0.018}}\sin\beta^{0.98}\cos\beta. \quad (10)$$

The Reynolds number is calculated using the equivalent diameter as a reference length:

$$Re = \frac{\rho U d_p}{\mu}. \quad (11)$$

To estimate the aerodynamic torque of the wings in the resting position (τ_w), we used a blade-element approach. We divided the length of the forewing (the hindwings are tucked under the forewings while in the resting position) into four sections (wing elements, Fig. 1C) and calculated the torque on each of the resulting elements independently of the other elements, under the quasi-steady assumption. We assumed that the aerodynamic force acts at the centroid of each wing element. The flow experienced at that point is due to the translation of the body in the direction of the jump (U) and the rotation of the wing about the pitch axis ($\dot{\boldsymbol{\theta}}_w\mathbf{r}$), where $\mathbf{r}$ is the vector connecting the centroid of the wing element with the center of mass.

The instantaneous aerodynamic force on the nth wing element (n=1,2,…4) was calculated as:

$$F_n = \frac{1}{2}\rho A_n C_{Fn}(\dot{\boldsymbol{\theta}}_w \mathbf{r}_n + \mathbf{U})^2 \sin\varepsilon, \quad (12)$$

where A_n is the planform area of the nth wing element, $\dot{\boldsymbol{\theta}}_w$ is the angular velocity of the wing about the pitch axis and C_{Fn} is the aerodynamic force coefficient.

For lack of concrete data, we used two alternative estimates for the force coefficient. First, we used the equations for the lift and drag coefficients of fruit-fly wings (Dickinson et al., 1999):

$$C_L = 0.225 + 1.58\sin(2.13\alpha - 7.20), \quad (13A)$$
$$C_D = 1.92 - 1.55\cos(2.04\alpha - 9.82), \quad (13B)$$

and found the aerodynamic force coefficient as:

$$C_F = \sqrt{C_D^2 + C_L^2}. \quad (13C)$$

In Eqns 13A and 13B, α is the instantaneous angle-of-attack of the wing-element with respect to the direction of flow in the pitch plane (measured in degrees). The calculated aerodynamic force (F_n, Eqn 12) is taken as perpendicular to the wing area (Dickson and Dickinson, 2004; Sane, 2003). Because this force estimate is for a fully deployed insect wing during flapping flight, we calculated a second (lower) estimate using the basic resistance of a plate with its broad side inclined into the flow using data provided in Hoerner (1965):

$$C_F = C_f + K\sin^3\beta, \quad (14A)$$

where C_f is the skin friction coefficient of a flat plate and K is the drag coefficient of a plate in normal (to the surface of the plate) flow. For conservative estimates of C_f and K at the appropriate Reynolds number (10<Re<50), we used:

$$C_f = \frac{1.328}{\sqrt{Re}}, \quad (14B)$$
$$K = 10.195Re^{-0.473}, \quad (14C)$$

where K is interpolated from fig. S26, page 3-15, in Hoerner (1965, see also page 2-4). The forces calculated using the low estimate are expected to designate the minimal force production by the closed wings.

We used the kinematic data from the movies with measurable wing supination (n=13) and by substituting either Eqn 14A or 13C into Eqn 12 we found in each movie frame the instantaneous force generated by the nth element. The instantaneous aerodynamic torque generated by this element is therefore:

$$\boldsymbol{\tau}_{w(n)} = \mathbf{r}_n \times \mathbf{F}_n. \quad (15)$$

The total instantaneous pitching torque from the wings is obtained by summing the torques from the four wing elements in each movie frame. Substituting the result (τ_w) in Eqn 5 with τ_b (Eqn 8) and the rotational damping coefficient (Eqn 7) gave the total pitching torque in air (τ_{pitch}). With the mass moment of inertia, Eqn 5 can be used to predict the instantaneous angular acceleration ($\ddot{\theta}$) of the body. To test the sensitivity of our model, we used the calculated estimates of torque to calculate the predicted angular acceleration of the body about the pitch axis. We used different values of I_{yy} for males and females based on intersexual differences in body mass and body length. We then averaged the predicted acceleration over time during the ballistic and wing supination phase in each take-off and compared it with the average angular accelerations measured from the movies. The latter was found by smoothing the instantaneous pitch angle data using a low-pass (300 Hz) Butterworth filter and finding the second derivative of the pitch angle with time (Rayner and Aldridge, 1985).

Throughout the paper, means are reported ±1 s.d.

RESULTS

In their resting position, the wings are pointing backwards along the sides of the insect, covering the dorsal and lateral sides of the abdomen like a gable roof (Figs 1, 2). The distal ends of the wings protrude a further 38±9.8% (n=10) of the body length beyond the posterior tip of the abdomen (Fig. 1). The wing center of area is located at 0.56±0.011 the distance from the wing base to the wing tip (wing length=0.91±0.125 mm), and coincides with the posterior tip of the abdomen (Fig. 1, n=16). Consequently, approximately half of the wing area and the maximal wing chord (located at 0.74±0.02 of the distance from the wing base to the tip, n=16) are located behind the posterior tip of the abdomen. The mean wing area was 0.58±0.072 and 0.39±0.079 mm^2 in females (n=20) and males (n=16), respectively. The supination of the wings (ε in Fig. 2A) in the resting position, as measured in the movies, was 31±7.2 deg (n=13).

The mean body length without the wings (B_L in Fig. 1B) was 0.81±0.106 mm (n=28), with a maximum width (lateral axis) and thickness (dorso-ventral axis) of 30±4.0% and 30±3.9% (n=10) of the body length, respectively. The body can be roughly divided along the longitudinal axis into two subunits: the head+thorax and the abdomen. The ellipsoids encompassing the two subunits are of similar volumes (ratio of 1.1:1; s.d.=0.32, n=10), suggesting that the center of mass is located at the junction between the thorax and the abdomen, which is located at 46±3.0% of B_L from the head (n=18). Females are slightly larger than males (m=41±11.9 and 25±5.7 µg, respectively, n=10 per sex; B_L=0.89±0.06 and 0.73±0.06 mm, n=15 and 13, respectively). As a result, the mean mass moment of inertia of females and males was 2.57×10^{-15} and 1.05×10^{-15} kg m^2, respectively. The average damping coefficient was calculated to be C_s=2.01×10^{-14} kg m^2 s^{-1}.

Take-offs

Out of 100 filmed take-offs, only nine showed wing flapping concurrent with the whitefly leaving the ground. In the remaining 91 (91%) take-offs, the whiteflies jumped into the air with their wings in the resting position. The hind legs were always the last to leave the ground. Fig. 2C shows the mean time allocation between the different phases in the take-off sequence. Wing flapping started in mid-air, 10.9±3.6 ms (n=74) after leaving the ground. The average 'ballistic' phase lasted 7.1±3.42 ms and wing deployment lasted 3.8±0.59 ms (n=73 and 81, respectively). By the time wing flapping started, the insects had reached a height above ground of 7.0±1.71 mm (i.e. 8.6 body lengths, n=34; Fig. 3). The mean speed at which the insects left the ground (take-off speed) was 0.61±0.097 m s^{-1}, and the average take-off angle was 64±10.7 deg (n=34). Table 1 summarizes the various kinematic parameters of the acceleration phase. The abrupt push against the ground resulted in a mean linear acceleration of 332.2±113.7 m s^{-2} (i.e. 34 times gravity) requiring a (body) mass-specific power output of 105.5±45.7 W kg^{-1} (n=27). When the whiteflies paused in preparation for jumping, their longitudinal axis was pitched upwards at an angle of 33±9.6 deg (n=32) relative to the horizontal plane (t_0 in Fig. 2B). During the acceleration phase, this angle decreased by 14±7.9 deg (n=32), suggesting a mean angular velocity of the body about the pitch axis of 22.9 Hz (i.e. revolutions s^{-1}, maximum observed=58.3 Hz). If the body had

Journal of Experimental Biology (2016) 219, 1639-1648 doi:10.1242/jeb.127886

Table 1. Summary of take-off performance

Measured parameter (units)	Calculation/ parameter	Mean±s.d.	*n*
Acceleration duration (ms)	$\Delta t=t_1-t_0$		
Measured at 2000 frames s^{-1}		1.7±0.28	77
Measured at 6000 frames s^{-1}		1.8±0.43	14
Take-off speed (m s^{-1})	$\lvert\mathbf{V}_0\rvert$	0.61±0.097	34
Mean acceleration during take-off (m s^{-2})	$\lvert\mathbf{V}_0\rvert/(t_1-t_0)$	332.2±113.7	27
Body pitch at t_0 (deg)	θ_{t_0}	33.9±9.61	32
Body pitch at t_1 (deg)	θ_{t_1}	18.8±12.49	32
Angular speed in the acceleration phase (deg s^{-1})	$\omega_0=(\theta_{t_1}-\theta_{t_0})/(t_1-t_0)$	8049±4898	32
Rotational kinetic energy (J)[a]	$W=0.5I_{yy}\omega^2$	$9.7\times10^{-11}\pm13.0\times10^{-11}$	32
Kinetic energy (J)[b]	$KE=0.5m\lvert\mathbf{V}_0\rvert^2$	$5.6\times10^{-9}\pm1.6\times10^{-9}$	34
Mass-specific power output (W kg^{-1})[c]	$KE/m\Delta t$	105.5±45.7	27
Take-off angle (deg)	γ	64±10.7	34

[a]Assuming constant angular acceleration, $\omega=2\omega_0$ and I_{yy} (for both males and females)=1.8×10^{-15} kg m^2.
[b]Assuming body mass (m)=30 µg. The mean body mass of 10 males and 10 females, measured with a microbalance.
[c]The calculation of (body) mass-specific power output neglects the rotational kinetic energy, which was two orders of magnitude lower than the linear kinetic energy.

continued to rotate in the air at the same average speed, it should have rotated another 90 deg in the 10.9 ms between leaving the ground and the initiation of flapping (t_4-t_1), resulting in the insect moving through air upside-down. The whiteflies did indeed pitch forward after leaving the ground (Fig. 4A), but only by 34±24.9 deg on average (maximum=100 deg, minimum=2 deg, n=32). The pitch angle of the body (θ) at the start of the acceleration phase (at t_0) and at leaving the ground (at t_1) were positively correlated (linear regression, r=0.77, P<0.001, n=32), and the difference between the two angles ($\theta_{t_0}-\theta_{t_1}$) was negatively correlated with the minimum (negative) pitch angle reached in the air (r=−0.9, P<0.001, n=32). The minimum pitch angle reached in the air did not show a significant correlation with the pitch angle at t_0 (P=0.7), but did show a weak positive correlation with the pitch angle at t_1 (r=0.5, P=0.004, n=32).

Body rotation in the air abruptly slowed down and reversed direction during wing deployment (Fig. 4). However, a close examination of the curves in Fig. 4 revealed that in more than half of the trials (66%), body rotation slowed down to a halt even before wing deployment initiated. Within these trials, in 10 cases (31% of the total take-offs) body rotation even reversed direction prior to wing deployment. The mean angular accelerations differed significantly between the 'acceleration', 'ballistic', 'supination' and 'elevation' phases (one-way ANOVA for repeated measurements, P<0.001). The forward pitch rotation speed of the body increased during the

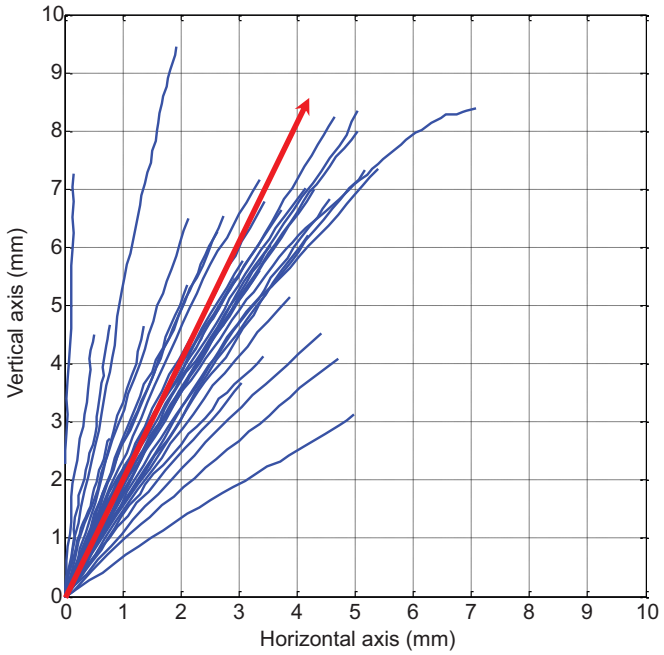

Fig. 3. Take-off trajectory and take-off angle. Each blue line denotes the position of the center of mass in air during a single take-off jump (during t_1-t_4). The red arrow denotes the mean jump angle (n=34). The take-off trajectory data of each jump were used to determine the take-off speed and direction.

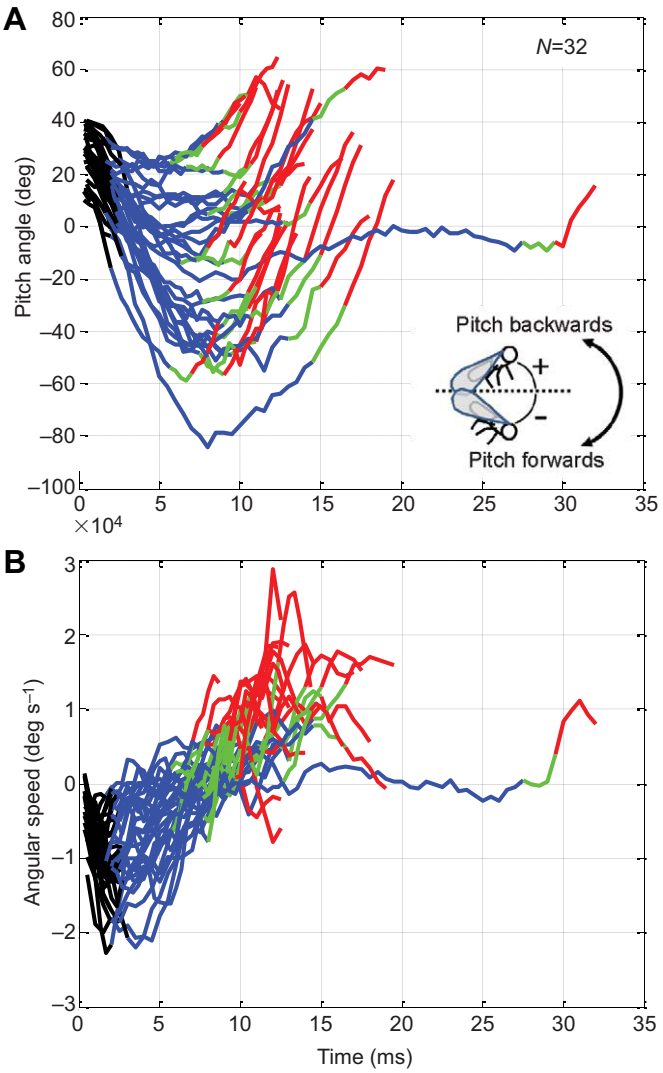

Fig. 4. Aerial righting during take-off. Change in pitch angle (A) and angular speed for pitch rotation (B) with time during the take-off sequence. Each curve represents a single take-off, with black denoting the 'acceleration' phase, blue the 'ballistic' phase, green the 'supination' phase and red the wing 'elevation' phase. Note that the time axis here starts at the first movement of the body (i.e. at t_0). The inset in A denotes the definition of positive and negative pitch angles and the terms (forward, backwards) used to describe pitching direction.

Journal of Experimental Biology

Journal of Experimental Biology (2016) 219, 1639-1648 doi:10.1242/jeb.127886

'acceleration' phase (mean acceleration $-2.6\times10^6\pm2.16\times10^6$ deg s^{-2}, n=32; see Fig. 4A for definition of rotation directions). The rotation speed slowed down and then accelerated in the opposite direction during the 'ballistic', 'supination' and 'elevation' phases (mean angular accelerations: $1.6\times10^6\pm0.83\times10^6$, $3.6\times10^6\pm2.42\times10^6$ and $0.5\times10^6\pm1.72\times10^6$ deg s^{-2}, respectively). The mean angular acceleration during the 'supination' phase was significantly higher than during the 'ballistic' and 'elevation' phases (Tukey's test, P<0.001).

Whiteflies with removed wings continued to rotate forward about the pitch axis after 15 ms from leaving the ground (Fig. 5A). Whiteflies with the distal half of their wings removed attempted to deploy their wings, but wing deployment did not result in the rapid backward pitch as in whiteflies with wings intact (Fig. 5B).

In insects with wings intact, supinating the wings in the resting position while the body moved through air (linear translation and rotation about the pitch axis) increased the projection of the wing area onto the flow (A'), as shown in Fig. 6A. Note that by the end of the supination phase (but prior to wing elevation) most of the wing area is perpendicular to the direction of motion in air. The calculated estimates from the biomechanical model (Fig. 6B,C) suggested that, once airborne, the aerodynamic torque acting on the closed wings

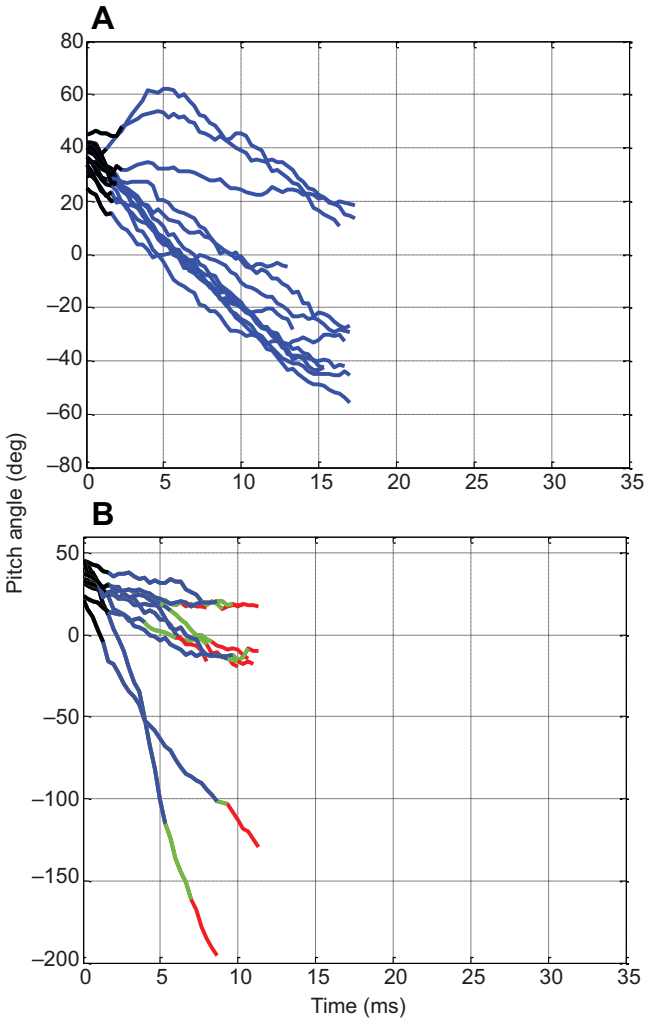

Fig. 5. Change in pitch angle with time during the take-off sequence for whiteflies. (A) Removed wings. (B) Clipped wings. The color code and time axis is the same as in Fig. 4. The curves in A and B denote 13 and 10 take-off jumps made by seven and nine different whiteflies, respectively.

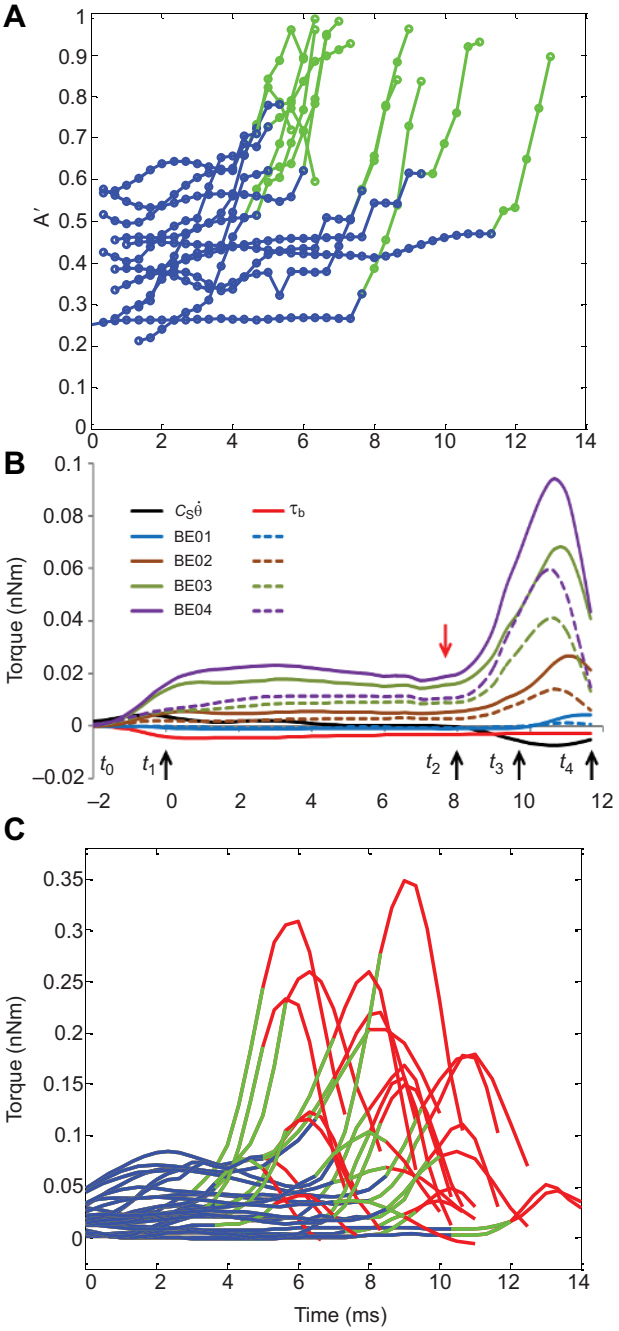

Fig. 6. Aerodynamic torque estimates from the model. (A) Change in projected wing area (A') during the ballistic (blue) and supination (green) phases. Each curve represents a single take-off jump for which the supination angle could be measured in the movies (n=13). (B) The model's estimate of the aerodynamic torque of a single take-off jump. Shown are the instantaneous torques due to motion of the body (Stokes' rotational damping and pitching torque) and the contribution of the four blade elements (BE01–04; see also Fig. 1C). Solid and dashed lines represent the calculation using the high and low estimates, respectively. Black arrows represent the transition between the various phases in the take-off sequence (t_0–t_4; see Fig. 2B for definitions). Red arrow denotes the instant when rotation of the body came to a stop. (C) Total torque estimated from the model using the higher estimates. Each curve represents a take-off sequence and the color code denotes the phase in the take-off section as in Fig. 4.

Journal of Experimental Biology

Journal of Experimental Biology (2016) 219, 1639-1648 doi:10.1242/jeb.127886

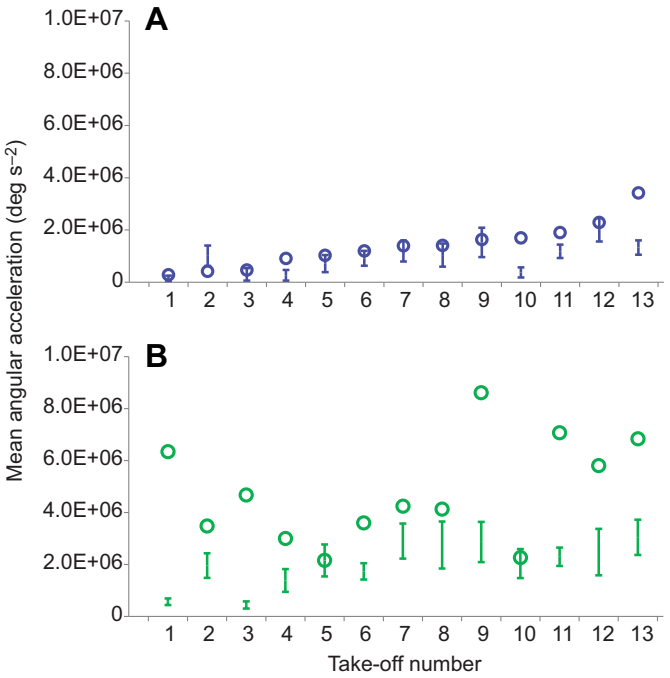

Fig. 7. Mean angular acceleration about the pitch axis in whiteflies during jumping. (A) Ballistic phase. (B) Supination phase. Shown are averages measured for each jump (circles) and estimates predicted by the biomechanical model (vertical bars). The bars denote the range between the high and low estimates for the same take-off sequence (n=13). The jumps are ordered in increasing order according to the observed acceleration during the ballistic phase.

was an order of magnitude higher than the torque acting on the body without the wings (Fig. 6B). Fig. 6B also illustrates the instantaneous aerodynamic pitching moments contributed by each of the four sections of the wings (BE01–04, see Fig. 1C). The two distal (posterior) sections of the closed wings together provided 89±2.3% and 87±6.9% out of the total torque from the wings for the high and low estimate, respectively. The total pitching torque (τ_{pitch}) became positive immediately at take-off, well in advance of the wing supination and elevation that occurred during wing deployment (Fig. 6C). However, during wing deployment, the magnitude of aerodynamic torque increased sharply (Fig. 6B,C), resulting in the sharp change in pitch angle of the body (Fig. 4B).

During the ballistic phase, the observed angular accelerations were significantly higher (paired t-test, P<0.001) and not different (paired t-test, P=0.46) than the predicted values derived from our model using the lower and higher estimates, respectively (Fig. 7A). The correlation between the predicted and observed accelerations was weak but significant (lower estimate: r=0.71, P=0.007; higher estimate: r=0.59, P=0.034). During the wing supination phase, the observed angular accelerations were significantly higher than both estimates (paired t-test, lower estimate: P<0.001; higher estimate: P=0.002; Fig. 7B) and there was no correlation between the observed angular accelerations and the angular accelerations predicted by the model (r<0.27, P>0.37 for both the lower and higher estimates).

DISCUSSION

Our whiteflies used only leg thrust to power take-offs in 91% of the trials, and the wings were deployed only after the insect moved several body lengths in the air. Weber (1931), who worked on greenhouse whiteflies (*Trialeurodes vaporariorum*), noted that the hind legs were capable of synchronized action to enable jumping. He further noted that the muscles powering the jumps were located inside the metathorax, and that whiteflies taking off from the underside of horizontal surfaces (e.g. leaves) fall 2–3 cm prior to opening their wings and flying. Our study, which focused on the tobacco whitefly (*B. tabaci*), corroborates Weber's observations and expands them to take-offs from the upper side of horizontal surfaces.

We hypothesized that in such take-off jumps, the rapid transition from ground to flapping flight would require one of three alternative take-off stabilization strategies: (1) the insect pushes against the ground with minimal body rotation, (2) rotations resulting from the push against the ground would be countered in the air by the flapping wings, or (3) the rotations would be countered in the air prior to wing flapping. Our measurements of timing of body rotation in the air (Fig. 4) support the third scenario, because the insects were capable of stopping body rotation prior to deploying and flapping their wings in 66% of the take-off jumps. In 31% of the jumps the insect even reversed the direction of body rotation prior to deploying their wings. However, it is also evident that wing deployment (supination and elevation) in itself provides a significant increase in torque, which reversed the direction of body rotation in the remaining trials, pitching the insect backwards into a posture more suitable for flight.

The acceleration phase sends the insects into the air rotating

The acceleration phase was extremely short (1.7 ms on average) yet delivered high acceleration of the body (on average, 34 times gravity, power output: 105 W kg^{-1} body mass; see Table 1). This supports the notion that *B. tabaci* utilize an elastic mechanism when jumping. Furthermore, the insects were immobile immediately prior to the acceleration phase, which may indicate that slow muscle work was taking place to store elastic energy in the body, locking some of the joints of the jumping mechanism and rendering the hind legs motionless.

One of the costs of a jumping mechanism based on abrupt release of stored energy is that it can send the body into the air rotating in an uncontrolled manner. Indeed, our whiteflies launched into the air rotating forward about the pitch axis. This occurred even when the analyzed take-offs were voluntary, executed from a flat and even surface, and the insects were uninterrupted as they prepared for take-off. Thus, the observed forward rotation of the body in the sagittal plane seems to be inherent to the take-off mechanism. The rotation likely resulted from the point of contact between the hind legs and ground being located posterior to the center of mass. As the hind legs pushed down against the ground, the resulting torque rotated the body forward in the pitch plane (Fig. 8). Once the body left the ground, the leg torque ceased to exist, but the body continued to rotate because of its angular momentum (Fig. 8B). Indeed, we found that the ballistic phase started with a high angular velocity (up to 58 revolutions s^{-1}, or 58 Hz) and that the minimum pitch angle achieved in the air was correlated with the rotation of the body during the acceleration phase.

Pitch rotation is dampened by the aerodynamics of the closed wings

Once in the air, during the ∼11 ms of air travel prior to the first downstroke, the body rotation decelerated and even reversed direction (Fig. 4). Because the insects were no longer in contact with the ground, any external stabilizing torque to resist the rotation of the body must have been due to aerodynamic force. During the

Journal of Experimental Biology (2016) 219, 1639-1648 doi:10.1242/jeb.127886

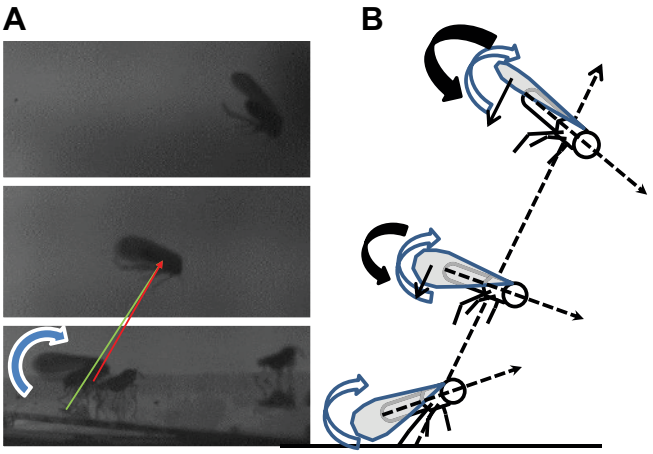

Fig. 8. Graphical summary of the proposed mechanism of aerial righting. (A) Three video frames from a single high-speed video laid one on top of the other to show a whitefly before leaving the ground and several body lengths into the air. The red arrow connects the center of mass on the ground and in the air. The green arrow connects the last point of contact on the ground and the center of mass in the air. The difference between the two lines on the ground emphasizes the forward pitching moment generated at take-off (thick blue arrow). Note the pitch of the body once in the air. (B) An illustration (not to scale) showing the point of contact with the ground being posterior to the center of mass, resulting in a forward pitch rotation (open curved arrow, here clockwise). Dashed arrows represent the longitudinal axis of the body. Straight black arrows represent the air resistance on the posterior end of the wings, and the curved black arrows represent the resulting aerodynamic torque operating counter to the rotation of the body (counterclockwise), slowing down the rotation.

ballistic phase, this aerodynamic force acts on the closed wings and on the rest of the body, but the quasi-steady blade-element model suggests that, by far, the closed wings provide most of the stabilizing torque (Fig. 6B). The fact that insects with removed wings continued to rotate in air (Fig. 5) supports this suggestion. Moreover, the model predicts that more than 87% of the stabilizing torque generated by the wings is generated by the distal half of the closed wings (Fig. 6B), which extends behind the posterior tip of the abdomen. Indeed, when only the distal section of the wings was trimmed, the insects did not stabilize body pitch during the jump. Hence, experiments as well as biomechanical considerations suggest that the wings play a substantial role in stabilizing body pitch before and during wing deployment. During the ballistic phase, the distal sections of the wings essentially operate as a posterior stabilizing surface resisting the rotation of the body. During wing deployment, the wings are rotated (supinated and elevated) to increase air resistance, further contributing to pitching the body backwards.

Such a function is performed by birds and man-made flyers using horizontal tails, located posterior to the center of mass, allowing some control over the pitch of the flyer. Insects do not have tails, and instead they use the forces generated by their flapping wings to dynamically stabilize their body orientation (Ristroph et al., 2013; Truong et al., 2014). Yet, when the wings are closed, dynamic stabilization is impaired. Ristroph et al. (2013) showed that the flight of fruit flies deprived of sensory data became unstable. The instability could be rectified by adding fibers to increase the drag on the posterior tip of the body, thus providing passive stability for pitch. Brackenbury (1996) noted that during jumping with the wings closed, the rotation rate of three homopteran species was low (5–9 Hz) compared with that of coleopteran flea beetles (35–187 Hz). He suggested that the relatively long wings of leafhoppers exert a stabilizing effect on body pitch when closed, by acting like 'the tail-fin of an aircraft'. Our study of *B. tabaci* provides evidence for passive stability by the close wings during the ballistic phase. In more than half of the cases, the insects were able to stop the high angular velocity of the body even while the wings were in the resting position. The area of a wing pair is 3.2-fold the planform (in the frontal plane) area of the body. Therefore, aerodynamic forces on the large flat wings can greatly exceed air resistance on the elliptically shaped body. Furthermore, because of the shape and size of the wings, the maximal wing chord and half of the wing area are posterior to the tip of the abdomen (Fig. 1), so that the aerodynamic force on the distal ends of the wings can result in substantial pitching torque at the center of mass. As the wings supinated, the insects rotated and the wings elevated, the area of the wings projected onto the flow increased, and so did the aerodynamic torque that countered the forward rotation of the body (Fig. 8).

The simplistic biomechanical model underestimated the angular accelerations observed during the supination phase (Fig. 7B). On average, the angular acceleration predicted by the model using the higher estimate was only 63±34.8% of the observed value (n=13) and there was no correlation between the predicted and observed values. This may be due to the fact that wing supination was much shorter (1.6 ms; Fig. 2) and immediately followed by wing elevation. Thus, internal torques, resulting from small movements of the wings and abdomen relative to the thorax, may be at play during the end of the supination phase, and these were unaccounted for in our model. Indeed, the wing elevation phase was associated with a rapid pitch of the body backwards (Fig. 4). Wing elevation may contribute to rotating the body in a second mechanism that is not accounted for in our aerodynamic model. Namely, the inertia from rotation of the wings (and added mass of air) about the hinges in the pitch plane can result in counter-pitch rotation of the body backwards. The delicate, small wings of whiteflies precluded the measurement of mass distribution along the wing and therefore wing inertia is not accounted for in our model. However, the effect of wing inertia and internal torques, if substantial, would only apply at wing deployment and will only add to the aerodynamic effect already described by our model.

The wing tips of many homopteran insects substantially extend behind the posterior tip of the abdomen, and some of these insects are also known to be prominent jumpers. It would therefore be interesting to examine how common this longitudinal stability mechanism is in other insects that power take-off with their legs while the wings are in the resting position.

Acknowledgements
We thank J. Byres and S. Naranjo from the USDA, Western Region Biomass Research Center, for providing body mass measurements of male and female whiteflies. We thank N. Paz for English editing and A. Ayali for suggesting improvements to the manuscript. We also thank the staff of the I. Meir Segals Garden for Zoological Research for logistical assistance.

Competing interests
The authors declare no competing or financial interests.

Author contributions
G.R. and D.G. conceived the idea for the study; G.R. and E.D. conducted the experiments and analyzed the data; D.G. and G.R. provided materials; G.R. and D.G. wrote the paper.

Funding
This research received no specific grant from any funding agency in the public, commercial, or not-for-profit sectors.

Supplementary information
Supplementary information available online at
http://jeb.biologists.org/lookup/suppl/doi:10.1242/jeb.127886/-/DC1

References

Bennet-Clark, H. C. (1975). The energetics of the jump of the locust *Schistocerca gregaria*. *J. Exp. Biol.* **63**, 53-83.

Bennet-Clark, H. C. and Lucey, E. C. (1967). The jump of the flea: a study of the energetics and a model of the mechanism. *J. Exp. Biol.* **47**, 59-67.

Bimbard, G., Kolomenskiy, D., Bouteleux, O., Casas, J. and Godoy-Diana, R. (2013). Force balance in the take-off of a pierid butterfly: relative importance and timing of leg impulsion and aerodynamic forces. *J. Exp. Biol.* **216**, 3551-3563.

Blackmer, J. L. and Byrne, D. N. (1993). Flight behaviour of *Bemisia tabaci* in a vertical flight chamber: effect of time of day, sex, age and host quality. *Physiol. Entomol.* **18**, 223-232.

Brackenbury, J. (1996). Targetting and visuomotor space in the leaf-hopper *Empoasca vitis* (Gothe) (Hemiptera: Cicadellidae). *J. Exp. Biol.* **199**, 731-740.

Brackenbury, J. and Wang, R. (1995). Ballistics and visual targeting in flea-beetles (Alticinae). *J. Exp. Biol.* **198**, 1931-1942.

Burrows, M. (2003). Biomechanics: Froghopper insects leap to new heights. *Nature* **424**, 509.

Burrows, M. (2007). Kinematics of jumping in leafhopper insects (Hemiptera, Auchenorrhyncha, Cicadellidae). *J. Exp. Biol.* **210**, 3579-3589.

Burrows, M. (2012). Jumping mechanisms in jumping plant lice (Hemiptera, Sternorrhyncha, Psyllidae). *J. Exp. Biol.* **215**, 3612-3621.

Burrows, M. and Dorosenko, M. (2014). Jumping mechanisms in lacewings (Neuroptera, Chrysopidae and Hemerobiidae). *J. Exp. Biol.* **217**, 4252-4261.

Byrne, D. N. (1991). Whitefly biology. *Annu. Rev. Entomol.* **36**, 341-357.

Card, G. M. and Dickinson, M. H. (2008). Performance trade-offs in the flight initiation of *Drosophila*. *J. Exp. Biol.* **211**, 341-353.

Christian, E. (1978). The jump of the springtails. *Naturwissenschaften* **65**, 495-496.

Dickinson, M. H. (1999). Haltere-mediated equilibrium reflexes of the fruit fly, *Drosophila melanogaster*. *Philos. Trans. R. Soc. B. Biol. Sci.* **354**, 903-916.

Dickinson, M. H., Lehmann, F. O. and Sane, S. P. (1999). Wing rotation and the aerodynamic basis of insect flight. *Science* **284**, 1954-1960.

Dickson, W. B. and Dickinson, M. H. (2004). The effect of advance ratio on the aerodynamics of revolving wings. *J. Exp. Biol.* **207**, 4269-4281.

Evans, M. E. G. (1972). The jump of the click beetle (Coleoptera, Elateridae)-a preliminary study. *J. Zool.* **167**, 319-336.

Fry, S. N., Sayaman, R. and Dickinson, M. H. (2003). The aerodynamics of free-flight maneuvers in *Drosophila*. *Science* **300**, 495-498.

Furth, D. G., Traub, W. and Harpaz, I. (1983). What makes *Blepharida* jump ? A structural study of the metafemoral spring of a flea beetle. *J. Exp. Zool.* **227**, 43-47.

Gronenberg, W. (1996). Fast actions in small animals: springs and click mechanisms. *J. Comp. Physiol. A* **178**, 727-734.

Hedrick, T. L. (2008). Software techniques for two- and three-dimensional kinematic measurements of biological and biomimetic systems. *Bioinspir. Biomim.* **3**, 034001.

Heitler, W. J. (1974). The locust jump: specialisations of the metathoracic femoral-tibial joint. *J. Comp. Physiol.* **89**, 93-104.

Hoerner, S. F. (1965). *Fluid-Dynamic Drag*. Bakersfield, CA: Hoerner Fluid Dynamics.

Isaacs, R., Willis, M. A. and Byrne, D. N. (1999). Modulation of whitefly take-off and flight orientation by wind speed and visual cues. *Physiol. Entomol.* **24**, 311-318.

Marden, J. H. (1987). Maximum lift production during takeoff in flying animals. *J. Exp. Biol.* **130**, 235-238.

Patek, S. N., Dudek, D. M. and Rosario, M. V. (2011). From bouncy legs to poisoned arrows: elastic movements in invertebrates. *J. Exp. Biol.* **214**, 1973-1980.

Pond, C. M. (1972). The initiation of flight in unrestrained locusts, *Schistocerca gregaria*. *J. Comp. Physiol.* **80**, 163-178.

Provini, P., Tobalske, B. W., Crandell, K. E. and Abourachid, A. (2012). Transition from leg to wing forces during take-off in birds. *J. Exp. Biol.* **215**, 4115-4124.

Rayner, J. M. V. and Aldridge, H. D. J. N. (1985). Three-dimensional reconstruction of animal flight paths and the turning flight of microchiropteran bats. *J. Exp. Biol.* **118**, 247-265.

Ribak, G., Pitts, M. L., Wilkinson, G. S. and Swallow, J. G. (2009). Wing shape, wing size, and sexual dimorphism in eye-span in stalk-eyed flies (Diopsidae). *Biol. J. Linn. Soc.* **98**, 860-871.

Ribak, G., Gish, M., Weihs, D. and Inbar, M. (2013). Adaptive aerial righting during the escape dropping of wingless pea aphids. *Curr. Biol.* **23**, R102-R103.

Ristroph, L., Bergou, A. J., Ristroph, G., Coumes, K., Berman, G. J., Guckenheimer, J., Wang, Z. J. and Cohen, I. (2010). Discovering the flight autostabilizer of fruit flies by inducing aerial stumbles. *Proc. Natl. Acad. Sci. USA* **107**, 4820-4824.

Ristroph, L., Ristroph, G., Morozova, S., Bergou, A. J., Chang, S., Guckenheimer, J., Wang, Z. J. and Cohen, I. (2013). Active and passive stabilization of body pitch in insect flight. *J. R. Soc. Interface* **10**, 20130237.

Sane, S. P. (2003). The aerodynamics of insect flight. *J. Exp. Biol.* **206**, 4191-4208.

Schmidt-Nielsen, K. (1997). *Animal Physiology. Adaptation and Environment*. Cambridge: Cambridge University Press.

Thomas, A. L. R. and Taylor, G. K. (2001). Animal flight dynamics I. Stability in gliding flight. *J. Theor. Biol.* **212**, 399-424.

Tobalske, B. W., Altshuler, D. L. and Powers, D. R. (2004). Take-off mechanics in hummingbirds (Trochilidae). *J. Exp. Biol.* **207**, 1345-1352.

Truong, T. Q., Phan, V. H., Sane, S. P. and Park, H. C. (2014). Pitching moment generation in an insect-mimicking flapping-wing system. *J. Bionic Eng.* **11**, 36-51.

Van Truong, T., Le, T. Q., Park, H. C., Yoon, K. J., Kim, M. J. and Byun, D. (2014). Non-jumping take off performance in beetle flight (rhinoceros beetle *Trypoxylus dichotomus*). *J. Bionic Eng.* **11**, 61-71.

Weber, H. (1931). Lebensweise und Umweltbeziehungen von *Trialeurodes vaporariorum* (Westwood) (Homoptera-Aleurodina). *Z. Morph. Ökol. Tiere* **23**, 575-753.

Zastawny, M., Mallouppas, G., Zhao, F. and Wachem, B. Van (2012). Derivation of drag and lift force and torque coefficients for non-spherical particles in flows. *Int. J. Multiph. Flow* **39**, 227-239.

Journal of Experimental Biology